

# Study of the structural evolution within polystyrene and polystyrene-gold composite colloidal crystals by atomic force microscopy and scanning electron microscopy

Simona Badilescu,<sup>a)</sup> Ahmad-Reza Hajiaboli, Nader Seirafianpour, Ramin Banan Sadeghian, Mojtaba Kahrizi, and Vo-Van Truong

Electrical and Computer Engineering Department, Concordia University, Montréal, Quebec, H3G 1A8, Canada

(Received 29 September 2006; accepted 8 December 2006; published online 11 January 2007)

The simultaneous presence of hexagonal and quadratic arrangements of polystyrene microspheres in the top layers of polystyrene and gold-polystyrene composite colloidal crystals has been evidenced by both atomic force microscopy and scanning electron microscopy. It is thought that the formation of layers with the two different packing modes is in agreement with the phase transformations found in systems with confined geometries. The results of this study are relevant to the fabrication of high quality photonic crystals. © 2007 American Institute of Physics. [DOI: 10.1063/1.2430934]

Monodisperse colloidal spheres are versatile building blocks for the fabrication of microstructures for photonic materials, sensors, and data storage devices. To obtain the desired structures, a number of techniques for self-assembly of colloidal particles have been explored over the past few years (Refs. 1–5 and references herein). As for gold composites, they are prepared, either by infiltrating a polystyrene (PS) template with gold<sup>6–9</sup> or by convective assembly of PS microspheres and gold nanoparticles.<sup>10</sup> The crystal formation is usually restricted to arrays of colloidal particles with a hexagonal orientation. Theoretical calculations have shown that a hexagonal-close-packed (hcp) structure is less stable compared to the face-centered-cubic (fcc) packing for particles with a hard-sphere potential. The free-energy difference between a fcc (ABCABC...) and hcp (ABABAB...) is around  $10^{-4}kT/\text{particle}$ .<sup>11</sup>

The first fluid-solid phase transitions in polystyrene suspensions confined between parallel glass plates were reported by Pieranski *et al.*<sup>12</sup> and van Winkle and Murray.<sup>13</sup> It was shown by Monte Carlo simulations<sup>14,15</sup> that confinement drastically affects the structure and the dynamical properties of the system.<sup>16</sup> Denkov *et al.*<sup>17</sup> and Dushkin *et al.*<sup>18</sup> signaled the evidence of small domains of square-packed particles at the boundary between the hexagonal mono- and bilayers in a cylindrical cell. The sequence of morphological transitions is the same as that observed by Pieranski *et al.*,<sup>12</sup> that is,  $1\Delta$ ,  $2\Box$ ,  $2\Delta$ ,  $3\Box$ ,  $3\Delta$ , ..., where the number denotes the number of layers and the symbol corresponds to layers of hexagonal ( $\Delta$ ) or square (quadratic) ( $\Box$ ) symmetry, respectively. The alternation of layers takes place in order to maximize the packing fraction ( $\Phi$ ) because of the smaller height of a fcc stack with quadratic (100) layers as compared to that of a hexagonal (111) stack.<sup>12</sup>

Our group has recently prepared and characterized PS-Au composite films deposited by convective assembly of PS and Au.<sup>19</sup> Here, we report on the atomic force microscopy (AFM) and scanning electron microscopy (SEM) observations of the simultaneous presence of hexagonal and quadratic arrangements of the microspheres in the top layers of PS and PS-Au films prepared by a vertical deposition

method. It is believed that the formation of the layers having different arrangements as seen in our experiments is in agreement with the phase transformations predicted in systems with confined geometries. The aim of this work is thus to understand the mechanism of layering transitions in the case of the convective self-assembly on vertical substrates by using the analytic capabilities of the AFM instruments.

The vertical deposition method used in this work is similar to the method employed by Denkov *et al.*<sup>17</sup> and Gu *et al.*<sup>20</sup> and the method of Yamaki *et al.*<sup>21</sup> PS microspheres (510 nm) or a mixture of 510 nm PS and 20 or 5 nm gold colloids has been used in all the experiments. The substrate was immersed vertically in the vial containing the PS suspension in water and was kept at 55–60 °C for at least 4 days.

Top-view AFM images recorded at different parts of the composite films clearly show an alternation of hexagonal and quadratic arrangements of the spheres. Figure 1 shows the AFM image of a composite film. The low magnification image [Fig. 1(a)] confirms that the film has a number of domains with different crystalline arrangements and orientations. The enlarged view of the area corresponding to the changing structure is given in Fig. 1(b). In the right part of this figure, a stripe of hexagonally arranged spheres is surrounded by two stripes of particles with a quadratic symmetry. The presence of a mixture of larger and smaller particles can be noticed. The figure also clearly shows the presence of both phases within a single array. We believe that this may be accounted for by the size polydispersity (SPD) that exists even to the most carefully prepared colloidal suspension. The effects of the particle size distribution on the kinetics of crystal nucleation and growth have been demonstrated both experimentally<sup>22</sup> and by computer simulation. It has been shown that, in a suspension with a broader SPD, the smaller particles (from the extremities of the SPD), due to their much higher diffusivity (which scales as  $R^3$ ), are directed toward the grain boundaries. If the crystal growth rate exceeds the diffusion rates of these particles, these latter may become trapped during solidification as it seems to be the case in our experiments.<sup>24</sup>

From these images, the change from quadratic to hexagonal and then back again to a quadratic structure would

<sup>a)</sup>Electronic mail: sbadiles@ece.concordia.ca

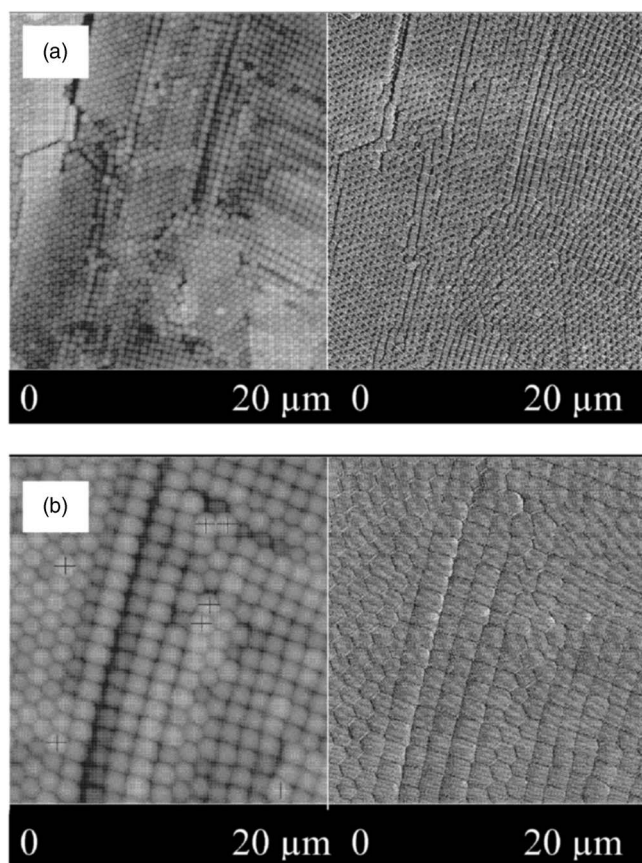


FIG. 1. AFM image of a PS-Au composite prepared by a vertical method. Large area view (a), enlarged image of (a) showing the changing structural arrangement (b), and surface plot (c). Some of the larger particles are marked by crosses in the image. Right hand images are phase images obtained in the tapping mode. They represent a combination diagram of the mechanical and topological properties of the surface under study.

take place in the same layer. However, the surface plot [Fig. 1(c)] reveals that at one of the boundaries there is a difference in the height of the particles, showing that at least one transition coincides with the formation of a new layer. The mean particle height in the hexagonal areas is found to be 195.8 nm and in the quadratic areas it is 99.4 nm. The sizes of the areas having different arrangements are irregular (widths in the range of 4–8  $\mu\text{m}$ ) and their shapes are random. Analysis of the AFM images shows that the mean roughness of the oven-deposited films is about 60 nm and the grain height is in the vicinity of 220 nm.

The AFM image of a PS colloidal crystal without Au insertion is given in Fig. 2. It can be seen that, while one of the scanned areas [Fig. 2(a)] shows a domain with an almost pure quadratic structure of the top layer, in another image, hexagonally packed spheres appear to be embedded in a quadratic crystallite [Fig. 2(b)]. The inset in Fig. 2(a) shows a magnified view of the cross section of the structure visible in the upper left corner. It reveals the presence of interlocked triangular shaped prisms with four spheres on each side. A similar pattern is shown by the SEM images of the PS colloidal crystal (Fig. 3). Figure 3(a) shows a multilayer structure with more than 15 layers and Fig. 3(b) reveals the alternation of the hexagonal and quadratic forms in three successive top layers. In Fig. 3(c), a succession of hexagonal-quadratic-quadratic layers is clearly seen.

Layered arrays are formed by convective transfer of particles from the bulk of suspension to the thin wetting film.

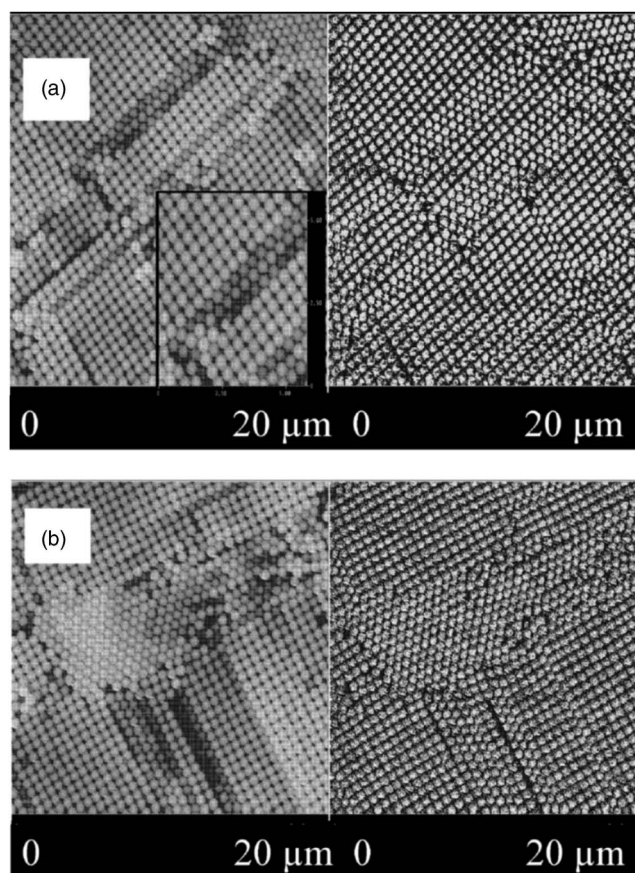


FIG. 2. AFM image of a PS colloidal crystal prepared under the same conditions as the composite film. The two images (a) and (b) correspond to two different areas of the sample. The inset in (a) shows the structure of the cross section.

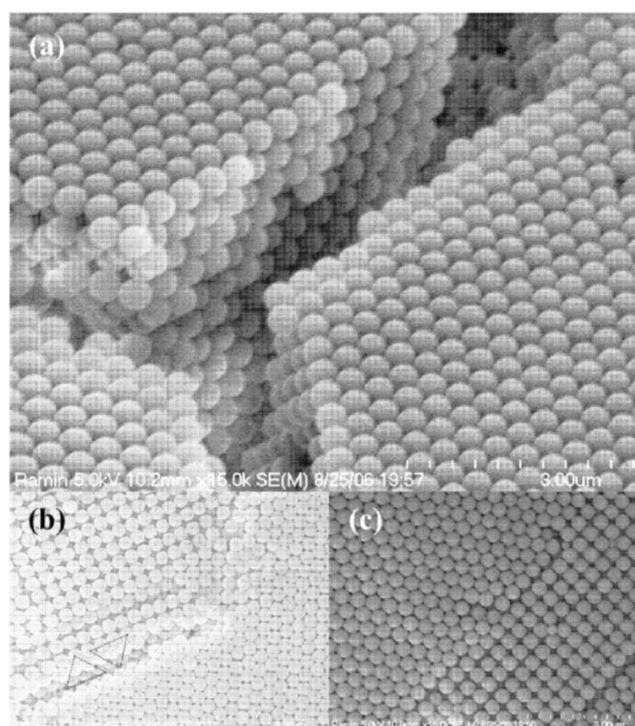


FIG. 3. SEM image of a PS colloidal crystal. The sample is viewed at 45° and the multilayers are seen along the cracks (a), quadratic and hexagonal arrangements of the spheres (b), and successive hexagonal-quadratic and hexagonal arrangements of spheres in the same layer (c).



Their transfer toward the meniscus is due to a pressure gradient caused by the water evaporation.<sup>17,23</sup> Due to hydrostatic pressure, the thickness of the wetting film increases from the meniscus downward toward the bulk suspension. The space between the substrate and the film surface may be considered a confined area that will be filled up by successive monolayers, bilayers, trilayers, etc., in the same way as in a thin wedge.<sup>24</sup> The alternation of hexagonal and quadratic packings of spheres is accounted for by the finite size effects arising from the confined geometry. The complexity of the layered structure in the case of the composite, as compared to the PS colloidal crystal, is accounted for by the influence of the gold nanoparticles on the phase transformations.

<sup>1</sup>O. D. Velev and A. M. Lenhoff, *Curr. Opin. Colloid Interface Sci.* **5**, 56 (2000).

<sup>2</sup>Nina V. Dziomkina and G. Julius Vancso, *Soft Mater.* **1**, 265 (2005).

<sup>3</sup>Zuocheng Zhou and X. S. Zhao, *Langmuir* **20**, 1524 (2004).

<sup>4</sup>Younan Xia, Byron Gates, Yadong Yin, and Yu Lu, *Adv. Mater. (Weinheim, Ger.)* **12**, 693 (2000).

<sup>5</sup>Mun Ho Kim, Sang Hyuk Imm, and Ok Park, *Adv. Funct. Mater.* **15**, 1329 (2005).

<sup>6</sup>P. Jiang, J. Cizeron, J. F. Bertone, and V. L. Colvin, *J. Am. Chem. Soc.* **121**, 7957 (1999).

<sup>7</sup>H. Yan, C. F. Blanford, B. T. Holland, M. Parent, W. H. Smyrl, and A.

Stein, *Adv. Mater. (Weinheim, Ger.)* **11**, 1003 (1999).

<sup>8</sup>O. D. Velev, P. M. Tessier, A. Lenhoff, and E. V. Kaler, *Nature (London)* **401**, 548 (1999).

<sup>9</sup>M. E. Abdelsalam, P. N. Bartlett, J. J. Baumberg, and S. Coyle, *Adv. Mater. (Weinheim, Ger.)* **16**, 90 (2004).

<sup>10</sup>P. M. Tessier, O. D. Velev, A. T. Kalambur, A. M. Lenhoff, J. F. Rabolt, and E. W. Kaler, *Adv. Mater. (Weinheim, Ger.)* **13**, 396 (2001).

<sup>11</sup>S. Pronk and D. Frenkel, *J. Chem. Phys.* **110**, 4589 (1999).

<sup>12</sup>P. Pieranski, L. Strzelecki, and P. Pansu, *Phys. Rev. Lett.* **50**, 900 (1983).

<sup>13</sup>D. H. van Winkle and C. A. Murray, *Phys. Rev. A* **34**, 562 (1983).

<sup>14</sup>M. Schmidt and H. Löwen, *Phys. Rev. E* **55**, 7228 (1997).

<sup>15</sup>R. Zangi and S. A. Rice, *Phys. Rev. E* **61**, 671 (2000).

<sup>16</sup>S. Naser, C. Bechinger, P. Leiderer, and T. Palberg, *Phys. Rev. Lett.* **79**, 2348 (1997).

<sup>17</sup>N. D. Denkov, O. D. Velev, P. A. Kralchevsky, I. B. Ivanov, H. Yoshimura, and K. Nagayama, *Langmuir* **8**, 3183 (1992).

<sup>18</sup>C. D. Dushkin, K. Nagayama, T. Miwa, and P. A. Kralchevsky, *Langmuir* **9**, 3695 (1993).

<sup>19</sup>S. Badilescu, M. Kahrizi, P. V. Ashrit, and Vo-Van Truong, *Proceedings of the Nanotech Conference, 2006*, pp. 293–296.

<sup>20</sup>Zhong-Ze Gu, Akira Fujishima, and Osamu Sato, *Chem. Mater.* **14**, 760 (2002).

<sup>21</sup>M. Yamaki, J. Higo, and K. Nagayama, *Langmuir* **11**, 2975 (1995).

<sup>22</sup>P. Jiang, J. F. Bertone, K. S. Hwang, and V. L. Colvin, *Chem. Mater.* **11**, 2132 (1999).

<sup>23</sup>S. I. Henderson, T. C. Mortensen, S. M. Underwood, and W. van Megen, *Physica A* **233**, 102 (1996).

<sup>24</sup>B. V. R. Tata, *Curr. Sci.* **80**, 948 (2001).